International Journal of Heat and Fluid Flow 44 (2013) 489–494

Contents lists available at ScienceDirect

International Journal of Heat and Fluid Flow

journal homepage: www.elsevier.com/locate/ijhff

Nusselt number and friction factor in thermally stratified turbulent channel flow under Non-Oberbeck–Boussinesq conditions

Francesco Zonta *

Centro Interdipartimentale di Fluidodinamica e Idraulica, Università degli Studi di Udine, Udine, Italy

ARTICLE INFO

Article history:
Received 17 April 2013
Received in revised form 19 July 2013
Accepted 8 August 2013
Available online 8 September 2013

Keywords:
Stratified flows
Turbulence
Numerical simulation

ABSTRACT

In stably stratified turbulence, computations under Oberbeck–Boussinesq (OB) hypothesis of temperature-independent fluid properties may lead to inaccurate representation of the flow field and to wrong estimates of momentum/heat transfer coefficients. This is clearly assessed here comparing direct numerical simulations of stratified turbulence under OB conditions to simulations under NOB (Non-Oberbeck–Boussinesq) conditions of temperature-dependent fluid viscosity and thermal expansion coefficient. Compared to the OB case, NOB conditions may induce local flow relaminarization with significant variations (up to 30%) of heat and momentum transfer coefficients. Together with DNS results, we propose a phenomenological model (based on turbulent bursts) for heat transfer prediction in stratified turbulence under OB and NOB conditions. Implications of NOB assumptions on mixing efficiency (i.e. flux Richardson number Ri_f) and turbulent Prandtl number (Pr_t) are also discussed. These results are of specific importance in RANS modelling, where the condition $Pr_t = 1$ is usually assumed (Reynolds analogy). Although this assumption is valid in some situations (i.e. boundary layer, pipe flow) there is uncertainty about its validity for stably-stratified turbulence. We demonstrate that this assumption is inaccurate when NOB effects become significant.

1. Introduction

Controlling momentum and heat transfer efficiency in stratified turbulence is of great importance in a wide range of industrial applications (Armenio and Sarkar, 2002). In many situations, stratification develops near a solid boundary: this is the case of heat exchangers, where stratification develops near their vertical/side boundaries. From a physical point of view, a wall-bounded stably stratified flow is a fluid layer confined between two conductive walls and heated from above (with gravity acting downwards in the wall-normal direction). The analysis of stably stratified flows is usually performed under the Oberbeck–Boussinesq (OB) approximation (Armenio and Sarkar, 2002; Iida et al., 2002), in which the fluid density depends linearly on temperature whereas all the other fluid properties are uniform and independent of temperature. However, the OB approximation is never exactly valid in practice, especially for liquids subjected to large temperature gradients (Ahlers et al., 2006). This is the case of water, for which fluid properties vary significantly with temperature. To fix reference values, when water temperature decreases from 343 K to 303 K, water viscosity changes from $\mu \simeq 0.4 \times 10^{-3}$ Pa s to $\mu \simeq 0.8 \times 10^{-3}$ Pa s, a value twice the size. For the same temperature variation, the thermal expansion coefficient decreases from $\beta \simeq 5.7 \times 10^{-4}\,\mathrm{K}^{-1}$ (at 343 K) to $\beta \simeq 3 \times 10^{-4}\,\mathrm{K}^{-1}$ (at 303 K), a value almost halved. Although NOB (Non-Oberbeck–Boussinesq) effects have been extensively investigated for Rayleigh–Benard convection (Ahlers et al., 2006; Sugiyama et al., 2009; Sameen et al., 2009), studies of NOB effects for stably-stratified flows are fewer (see Zonta et al., 2012b and references therein).

In this paper, we demonstrate that NOB assumptions lead to a symmetry breaking of the flow structure (the degree of asymmetry being dependent on the flow parameters) with significant modifications of momentum and heat transfer mechanisms. Implications of NOB assumptions on mixing efficiency (i.e. the amount of energy available for mixing which is irreversibly lost to potential energy, here quantified by the flux Richardson number Ri_f) and on the turbulent Prandtl number (Pr_t) are also discussed. These results are of importance for RANS modelling, where the Reynolds analogy ($Pr_t = 1$) is usually adopted. Although this assumption is valid in a variety of situations (i.e. boundary layer, pipe flow) there is uncertainty about its validity for stably-stratified turbulence (Laskowski et al., 2007). We demonstrate here that the Reynolds analogy is applicable only when OB conditions hold, but totally unphysical otherwise. In the latter case, more accurate physical modelling is required to improve current parametrization of mixing in stratified turbulence.

2. Formulation

We perform Direct Numerical Simulations (DNS) of an incompressible and Newtonian turbulent flow of water in a plane channel (with differentially-heated walls). Momentum and energy

* Tel.: +39 0432558006.
E-mail address: francesco.zonta@uniud.it

0142-727X/$ - see front matter © 2013 Elsevier Inc. All rights reserved.
http://dx.doi.org/10.1016/j.ijheatfluidflow.2013.08.007

balance equations are written in a variable-properties formulation and are solved using a pseudo-spectral technique (Zonta et al., 2012a,b). We consider the case of stably-stratified turbulence, consisting of a fluid layer confined between a hot top wall (kept at temperature θ_H) and a cold bottom wall (kept at temperature θ_C). The flow is driven by a pressure gradient in the horizontal direction, x (whereas gravity acts downward in the wall-normal direction, z). The problem of heat convection in stratified turbulence is described by the shear Reynolds number (Re_τ), the Grashof number (Gr) and the Prandtl number (Pr):

$$Re_\tau = \frac{\rho u_\tau h}{\mu}, \quad Gr = \frac{g\beta\Delta\theta(2h)^3}{\nu^2}, \quad Pr = \frac{\mu c_p}{\lambda}. \tag{1}$$

In Eq. (1), density (ρ), dynamic and kinematic viscosities (μ, ν), thermal conductivity (λ), specific heat (c_p) and thermal expansion coefficient (β) of the fluid are all evaluated at the reference temperature $\theta_{ref} = (\theta_H + \theta_C)/2$. Also, $u_\tau = \sqrt{\tau_w/\rho}$ is the shear velocity ($\tau_w = \mu\partial\langle u_x\rangle/\partial z$ being the shear stress at the wall and u_x the streamwise velocity), h is the half-channel height, g is the acceleration due to gravity and $\Delta\theta = \theta_H - \theta_C$ is the temperature difference between the walls. Brackets $\langle\cdot\rangle$ indicate average in time and in space (over the wall surfaces). The Reynolds and Grashof numbers quantify the importance of the inertial and buoyancy effects within the flow, whereas the Prandtl number is a property of the fluid state and measures the ratio between momentum and thermal diffusivity. In stratified flows, the behaviour of the flow field may be described by the shear Richardson number, $Ri_\tau = Gr/Re^2$. In this study we fix the value of Pr and Gr ($Pr = 3$ and $Gr \simeq 1.1 \times 10^7$) and we consider three different values of the shear Reynolds number: $Re_\tau = 110$, 150 and 180. This corresponds to a physical situation in which water at $\theta_{ref} = 50\,^\circ$C is used as working fluid and the temperature difference between the hot and cold wall is $\Delta\theta = 40\,^\circ$C. In the present study, we consider all fluid properties uniform but μ and β. Variations of ρ, λ and c_p with temperature are at least an order of magnitude lower and may be neglected (Incropera and Dewitt, 1985; Zonta et al., 2012b). To assess modifications of momentum and heat transfer coefficients due to NOB conditions, we compute the friction factor (C_f), the bulk Nusselt number (Nu_b) and the centreline Nusselt number (Nu_c) as:

$$C_f = \frac{\tau_w}{\frac{1}{2}\rho u_b^2}, \quad Nu_b = \frac{q_w D_h}{\lambda(\theta_W - \theta_b)}, \quad Nu_c = \frac{q_w h}{\lambda(\theta_W - \theta_{ref})}, \tag{2}$$

where $q_w = \lambda\partial\langle\theta\rangle/\partial z$ is the mean heat flux at the wall while u_b and θ_b are the bulk velocity and bulk temperature. Note that the bulk Reynolds number may be defined as $Re_b = \rho u_b D_h/\mu$, where $D_h = 4h$ is the hydraulic diameter.

3. Results

Measurements of friction factor (C_f) and Nusselt numbers (Nu_b and Nu_c) for the case of neutrally-buoyant channel turbulence (forced convection, *FC*, i.e. buoyancy is neglected) were performed to obtain reference data for benchmarking stratified turbulence results. Measured values are summarized in Table 1. Although buoyancy is neglected (neutrally-buoyant turbulence), NOB effects (due solely to $\mu(T)$ in this case) are anyway important at the Reynolds numbers considered in this study (Zonta et al., 2012a): the local value of the friction factor computed at the cold (C_f^C) and hot wall (C_f^H) is substantially different (±15%) from that obtained assuming uniform fluid properties (C_f). These differences are due to a different value of the shear stress at the two walls, which depends on the local value of the fluid viscosity. By contrast, the Nusselt number is not influenced by temperature-induced viscosity variations. This result can be explained considering that, in this specific flow configuration, the total heat flux is constant across the channel. In Table 1 we also provide reference data for C_f and Nu_b obtained from currently available correlations. In particular, we use $C_f = 0.073 \times Re_m^{-1/4}$ (Dean, 1978) and $Nu_b = 0.027 \times Re_b^{4/5} Pr^{1/3}$ (Sieder and Tate, 1936). Note that $Re_m = Re_b/2$.

Measurements of friction factor (C_f) and Nusselt numbers (Nu_b and Nu_c) for the case of stratified turbulence are shown in Figs. 1–3 and summarized in Table 2. In particular, in Fig. 1 the friction factor $C_f/C_{f,0}$ ($C_{f,0}$ being the friction factor for neutrally-buoyant flows) is computed as a function of the reference Ri_τ at the hot wall (open symbols) and at the cold wall (filled symbols). Depending on the value of Ri_τ, a peculiar range of influence of $\mu(T)$ and $\beta(T)$ is recognized: for larger Ri_τ (resp. smaller Ri_τ), $\mu(T)$ only (resp. $\beta(T)$ only) has an impact on momentum transfer efficiency. Although at higher Reynolds number (and lower Richardson number) the effect of $\mu(T)$ vanishes (Fig. 1a), the effect of $\beta(T)$ persists (Fig. 1b). There is a range of intermediate situations (corresponding here to $Ri_\tau = 498$ and $Re_\tau = 150$) in which the effects of $\mu(T)$ and $\beta(T)$ are both significant and comparable. We take this specific situation as reference case to discuss NOB effects on momentum/heat transfer efficiency. For $\mu(T)$ and $Ri_\tau = 498$ (Fig. 1a), $C_f/C_{f,0} \simeq 0.9$ at the hot wall and $C_f/C_{f,0} \simeq 0.4$ at the cold wall. Turbulence is sustained near the hot wall, where viscosity is lower, and suppressed near the cold wall, where viscosity is higher and flow relaminarization is observed (see inset of Fig. 1a). An opposite situation occurs when $\beta(T)$ is considered, with turbulence sustained near the cold wall only ($C_f/C_{f,0} \simeq 0.9$ at the cold wall and $C_f/C_{f,0} \simeq 0.4$ at the hot wall). This result is consistent with the distribution of β (and of the buoyancy force $F_B \propto \beta(T)$) across the channel. A fluid particle close to the hot wall experiences a buoyancy F_B which is larger than that of a fluid particle close to the cold wall, resulting in buoyancy-dominated laminar flow (buoyancy has a stabilizing effect) near the hot wall and shear-dominated turbulent flow near the cold wall. An instance of this peculiar flow configuration is shown in the inset of Fig. 1b.

The structure of the flow field also influences the average values of momentum/heat transfer. Compared to the neutrally-buoyant case ($C_{f,0}$,$Nu_{c,0}$) stable stratification reduces the average transport of momentum and heat (Arya, 1975; Armenio and Sarkar, 2002; Iida et al., 2002). The friction factor (C_f) and the Nusselt number (Nu) drop accordingly, while the bulk velocity increases (Table 2). To gain insight into the physical mechanism responsible for this behaviour, flow visualizations (contour maps of the temperature field) for neutrally-buoyant and stably stratified turbulence are presented and briefly discussed (Fig. 2). Simulations at $Re_\tau = 150$ are taken as reference case here. For stably-stratified turbulence (Fig. 2a) elongated wavy structures, called Internal Gravity Waves (IGW), are observed in the core region of the channel. For neutrally-buoyant turbulence (Fig. 2b), temperature is advected as a passive scalar and there is no physical mechanism (induced by the balance between inertia and buoyancy) for IGW to be sustained. It is clear that momentum and heat transfer are strongly influenced by IGW: fluid parcels that reach IGW do not have enough energy to penetrate them, since IGW create a strong temperature gradient (thermocline) which acts as a potential barrier (Ferziger et al., 2002; Zonta et al., 2012b). As a consequence, transfer coefficients reduce considerably. In Fig. 3 we quantify this trend. Note that for $Ri_\tau = 926$ the stabilizing effect of buoyancy is so overwhelming compared to inertia that the flow becomes laminar ($C_f/C_{f,0} \simeq 0.2$ and $Nu_c/Nu_{c,0} \simeq 0.12$). We also note that NOB effects (due to $\beta(T)$ in particular) on the overall momentum/heat transport efficiency may be important: compared to the OB case (–▼– in Fig. 3a), differences of Nu_c and C_f up to 25% are visible for $\beta(T)$ at $Ri_\tau = 346$ (–■– in Fig. 3a). Viscosity variations have a negligible influence on the overall momentum/heat transport efficiency. However, this average value hides the real physics of the phenomenon, characterized by a strongly non-symmetric flow behaviour (see Fig. 1 and comments therein). Flow asymmetry

Table 1
Friction factor (C_f) and Nusselt numbers (Nu_b,Nu_c) for turbulent Forced Convection (FC) in neutrally-buoyant channel flow. Simulations *FC*1 and *FC*2 are performed on a $128 \times 128 \times 129$ grid. Simulations from *FC*3 to *FC*6 are performed on a $256 \times 256 \times 257$ grid. When $\mu = \mu(T)$ friction factors C_f^H and C_f^C are evaluated at the hot and cold wall, respectively. Reference data from currently available correlations are also provided. In particular, we use $C_f = 0.073 \times Re_m^{-1/4}$ (Dean, 1978) and $Nu_b = 0.027 \times Re_b^{4/5} Pr^{1/3}$ (Sieder and Tate, 1936), where $Re_m = Re_b/2$.

Thermophysical properties	Re_τ	Re_b	C_f		C_f	Nu_b	Nu_b	Nu_c
			C_f^C	C_f^H [$\times 10^{-3}$]	(Dean, 1978) [$\times 10^{-3}$]		(Sieder and Tate, 1936)	
*FC*1: OB	110	6445	9.3		9.7	37.5	43.4	8.1
*FC*2: $\mu = \mu(T)$	110	6371	10.8	8.2	9.7	37.5	43	8.1
*FC*3: OB	150	9198	8.5		8.9	52	57.7	11.3
*FC*4: $\mu = \mu(T)$	150	9113	10.1	7.7	8.9	52.1	57.3	11.4
*FC*5: OB	180	11269	8.2		8.4	63.1	67.9	13.6
*FC*6: $\mu = \mu(T)$	180	11085	9.4	7.4	8.4	63	67.1	13.6

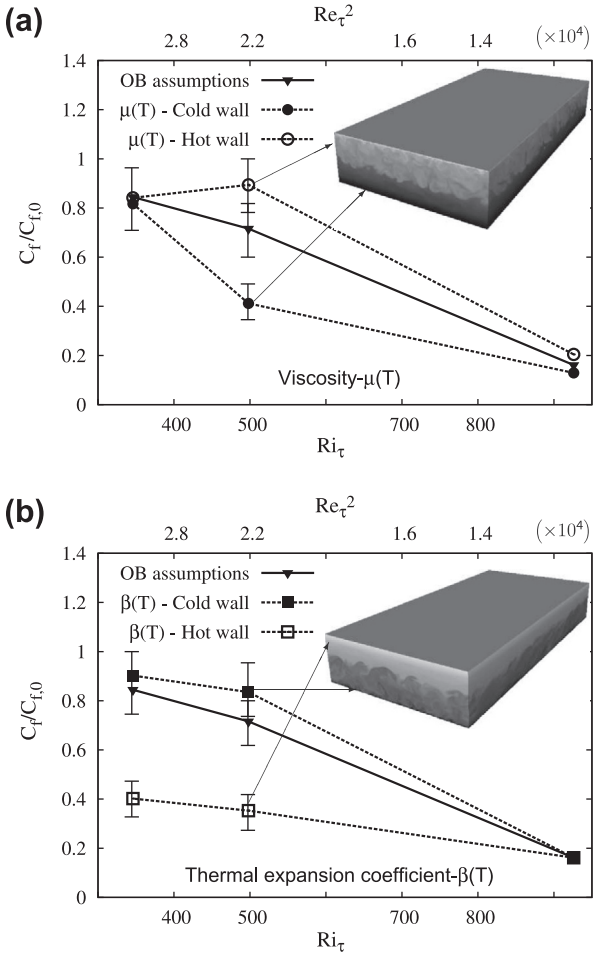

Fig. 1. (a) Normalized friction factor ($C_f/C_{f,0}$) for simulations with $\mu(T)$ computed at the hot and cold walls. (b) Normalized friction factor ($C_f/C_{f,0}$) for simulations with $\beta(T)$ computed at the hot and cold walls. Open symbols (–○– and –□–) represent the values of $C_f/C_{f,0}$ computed at the hot wall; close symbols (–●– and –■–) represent the values of $C_f/C_{f,0}$ computed at the cold wall. Values of $C_f/C_{f,0}$ obtained from OB simulations (–▼–) are also shown for comparison purposes. Flow visualizations using contour maps of the temperature field have been inserted (insets). Error bars represent the standard deviation of C_f from its averaged value.

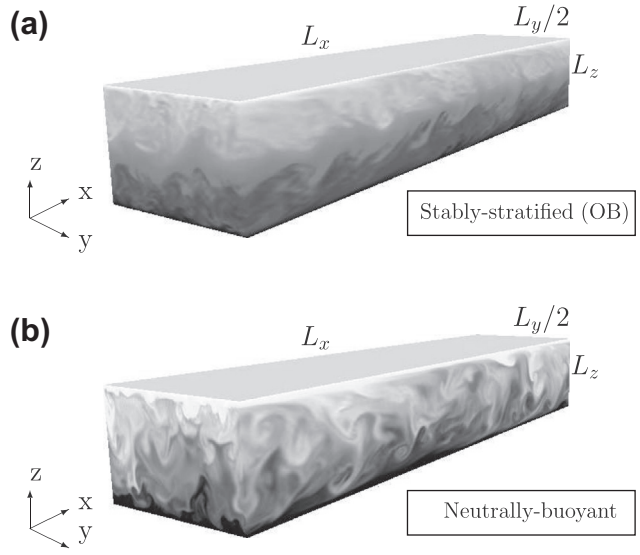

Fig. 2. (a) Contour maps of the temperature field for stably-stratified flow (OB assumptions) at $Re_\tau = 150$ (only half domain is shown along y direction). (b) Contour maps of the temperature field for neutrally-buoyant flow at $Re_\tau = 150$ (only half domain is shown along y direction).

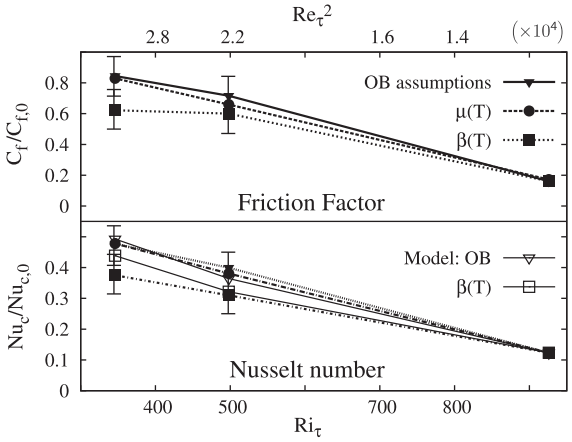

Fig. 3. Normalized friction factor ($C_f/C_{f,0}$) and Nusselt number ($Nu_c/Nu_{c,0}$) for simulations of stably-stratified turbulence: –▼– represents results obtained assuming OB assumptions; –●– represents results obtained assuming $\mu(T)$; –■– represents results obtained assuming $\beta(T)$. Results of $Nu_c/Nu_{c,0}$ obtained from our semplified model of heat transfer in stably stratified turbulence (open symbols) are also shown: –▽– for OB assumptions, –□– for $\beta(T)$. Error bars represent the standard deviation of C_f and Nu from their averaged value.

induced by the temperature dependence of the fluid properties (NOB effects) have been experimentally observed in Rayleigh–Benard convection (see Ahlers et al., 2009 for a review). However, in contrast to our findings, Nu in Rayleigh–Benard convection is surprisingly insensitive to NOB effects. We believe that this difference is due to flow configuration (Rayleigh–Benard convection in Ahlers et al. (2009), stratified channel turbulence in our work). In stratified channel turbulence, heat is driven by a combination of natural convection effects (due to temperature differences) and forced convection effects (due to the mean flow in the streamwise

Table 2
Friction factor (C_f) and Nusselt numbers (Nu_b,Nu_c) for turbulent convection in a stably-stratified channel flow. Simulations are performed on a 256 × 256 × 257 grid. When $\mu = \mu(T)$ friction factors C_f^H and C_f^C are evaluated at the hot and cold wall, respectively.

Thermophysical properties	Re_τ	Ri_τ	Re_b	C_f		Nu_b	Nu_c
				C_f^C	C_f^H [× 10^{-3}]		
*SS*1: OB	110	926	16112	1.5		6.4	1
*SS*2: $\mu = \mu(T)$	110	926	15255	1.2	1.9	6.4	1
*SS*3: $\beta = \beta(T)$	110	926	16130	1.5	1.5	6.4	1
*SS*4: OB	150	498	10919	6.1		36.2	4.5
*SS*5: $\mu = \mu(T)$	150	498	11338	3.5	7.6	35	4.3
*SS*6: $\beta = \beta(T)$	110	498	11900	7.1	3	28.7	3.5
*SS*7: OB	180	346	12280	6.9		50.4	6.5
*SS*8: $\mu = \mu(T)$	180	346	12312	6.7	6.9	50.1	6.5
*SS*9: $\beta = \beta(T)$	180	346	14322	7.4	3.3	39.2	5.1

direction). Since forced convection effects are negligible in Rayleigh–Benard convection, we might expect a different influence of NOB on *Nu* behaviour depending on the specific problem (Rayleigh–Benard convection, as in Ahlers et al. (2009), or stratified channel turbulence, as in the present work).

3.1. A phenomenological model for Nu prediction

Prediction of Nusselt number (*Nu*) in forced convection is a problem that has been extensively investigated in literature, and several numerical correlations have been developed (Sieder and Tate, 1936). By contrast, explicit correlations for predicting *Nu* in stratified turbulence are scarce. For this reason, we try to develop here a phenomenological model for heat transfer prediction in stratified turbulence. Our model is built following that of Hetsroni et al. (1996), developed for predicting heat transfer in forced-convection turbulence. Some of the details derived in Hetsroni et al. (1996) are recalled in the following for completeness. We have recently applied a similar strategy for *Nu* prediction in Poiseuille–Rayleigh–Benard turbulent flows (Zonta and Soldati, 2013). We assume that the amount of heat Q removed from the wall during time t is the sum of a conductive heat flux $Q1$ (quasi-laminar regions) and a convective heat flux $Q2$ (bursting events). Depending on the behaviour of the flow field, $Q1$ or $Q2$ may provide negligible contributions to Q: specifically, we can assume $Q \simeq Q1$ for laminar flows and $Q \simeq Q2$ for turbulent flows. We consider first the turbulent flow case. A bursting event (coherent structure) is modelled as an axially symmetrical submerged jet. The energy transferred from the wall by a submerged jet of cross-sectional area s and duration t_1 is (see Hetsroni et al., 1996) $Q = 2\rho c_p w_m \Delta\theta_m s\ t_1 I$, where $I \simeq A/Pr^n$ (for water, $A = 0.0667$ and $n = 0.8$), w_m and θ_m are the velocity and the temperature at the axis of the jet while $\Delta\theta_m = \theta_m - \theta_{ref}$ (θ_{ref} is the centerline reference temperature). For the present model, we assume that a fluid particle entrained in a burst event is driven by two opposite mechanisms: a shear-induced mechanism which pushes a particle away from the wall, and a buoyancy-induced mechanism which pushes a particle towards the wall (in stratified flows, a fluid particle that does get displaced away from the wall tends to be restored to its original position). Associated to these opposite mechanisms, we may define two different characteristic velocities, i.e. $w_{m,shear}$ and $w_{m,buoy}$ such that $w_m = w_{m,shear} - w_{m,buoy}$. Since the total amount of heat removed from the wall is $Q = \alpha(\theta_w - \theta_{ref})$, the thermal balance reads as:

$$Q = \alpha(\theta_w - \theta_{ref}) = 2\rho c_p (w_{m,shear} - w_{m,buoy})\Delta\theta_m \gamma (A/Pr^n), \tag{3}$$

with α the heat transfer coefficient and $\gamma = t_1/t$. In dimensionless form, obtained multiplying by $h/\lambda(\theta_w - \theta_{ref})$ and assuming $\Delta\theta_m = \theta_w - \theta_{ref}$, Eq. (3) becomes

$$Nu_c = \alpha h/\lambda = \underbrace{2\frac{\mu}{\nu}c_p w_{m,shear}\gamma\frac{A}{Pr^n}\frac{h}{\lambda}}_{Nu_{c,0}} - \underbrace{2\frac{\mu}{\nu}c_p w_{m,buoy}\gamma\frac{A}{Pr^n}\frac{h}{\lambda}}_{Nu_{c,buoy}}. \tag{4}$$

Based on Eq. (4), the Nusselt number may be considered as the sum of a contribution due to turbulent bursts ($Nu_{c,0}$, buoyancy is neglected) and a contribution due to buoyancy ($Nu_{c,buoy}$). Eq. (4) may be written as $Nu_c/Nu_{c,0} = 1 - w_{m,buoy}/w_{m,shear}$, where $w_{m,shear} = \epsilon u_b$ (with u_b the bulk velocity) and $w_{m,buoy} = (g\beta_{ref}\Delta\theta 2h)^{1/2} = 1/2 Gr^{1/2}\nu/h$ (i.e. the free-fall velocity, see Sugiyama et al., 2009). Since burst events originated in the near-wall region expand into the outer region with a wall-normal velocity comparable to the streamwise convection velocity, we assume $w_{m,shear} \simeq u_b$ and hence $\epsilon = 1$. For wall-bounded turbulent flows, the bulk velocity may be expressed as $u_b/u_\tau = 8.74 Re_\tau^{1/7}$ (Schlichting, 1979). With these assumptions, we obtain

$$\frac{Nu_c}{Nu_{c,0}} \simeq 1 - \frac{1}{17.4}\frac{Gr^{1/2}}{Re_\tau}\frac{1}{Re_\tau^{1/7}} = 1 - \frac{1}{17.4}\frac{Ri_\tau^{1/2}}{Re_\tau^{1/7}}. \tag{5}$$

For laminar flow (no contribution by turbulent bursts), we have $Nu_c = (\alpha h)/(\lambda) = (q_w h)/(\theta_w - \theta_{ref}) = 1$. For our simulations, $Nu_c/Nu_{c,0} \simeq 0.49$ (for $Ri_\tau = 346$ and $Re_\tau = 180$), $Nu_c/Nu_{c,0} \simeq 0.38$ (for $Ri_\tau = 498$ and $Re_\tau = 150$) and $Nu_c/Nu_{c,0} \simeq 0.12$ (for $Ri_\tau = 926$ and $Re_\tau = 110$). The present model may be extended to NOB conditions. In particular, when $\beta(T)$ is considered, the characteristic free-fall velocity should be corrected to represent the actual (vertical) velocity in a fluid layer with non-uniform β. Assuming $w_{m,buoy}^{NOB} = (\beta_{bulk}/\beta_{ref})^{1/2} w_{m,buoy}$, with β_{bulk} the bulk thermal expansion coefficient, we obtain

$$\frac{Nu_c}{Nu_{c,0}} \simeq 1 - \left(\frac{\beta_{bulk}}{\beta_{ref}}\right)^{1/2}\frac{1}{17.4}\frac{Ri_\tau^{1/2}}{Re_\tau^{1/7}}. \tag{6}$$

In our simulations $(\beta_{bulk}/\beta_{ref})^{1/2} = 1.1$, leading to $Nu_c/Nu_{c,0} \simeq 0.44$ (for $Ri_\tau = 346$ and $Re_\tau = 180$), $Nu_c/Nu_{c,0} \simeq 0.32$ (for $Ri_\tau = 498$ and $Re_\tau = 150$) and $Nu_c/Nu_{c,0} \simeq 0.12$ (for $Ri_\tau = 926$ and $Re_\tau = 110$). Values of Nu_c obtained from the present model for both OB (uniform fluid properties, $-\triangledown-$) and NOB ($\beta(T)$, $-\square-$) assumptions are shown in Fig. 3 together with our DNS results. A nice qualitative and quantitative agreement between DNS results and the simplified model is observed. For OB conditions, the present model works properly throughout the entire range of parameters considered in this study. For NOB conditions, the present model is still accurate except for $Ri_\tau = 346$, where some differences, compared to DNS results, are observed. In particular, this model seems to underestimate the stabilizing effect due to local flow relaminarization produced by temperature dependent thermal expansion coefficient at $Ri_\tau = 346$.

3.2. Mixing efficiency and turbulent Prandtl number

We conclude our analysis considering NOB effects on flow mixing efficiency and on turbulent Prandtl number. For stably stratified shear flows, mixing efficiency can be evaluated from the flux Richardson number Ri_f (Peltier and Caulfield, 2003):

$$Ri_f = \frac{B_k}{P_k} = \frac{g\beta\langle\theta' u_z'\rangle}{\langle u_x' u_z'\rangle\frac{\partial\langle u_x\rangle}{\partial z}}, \tag{7}$$

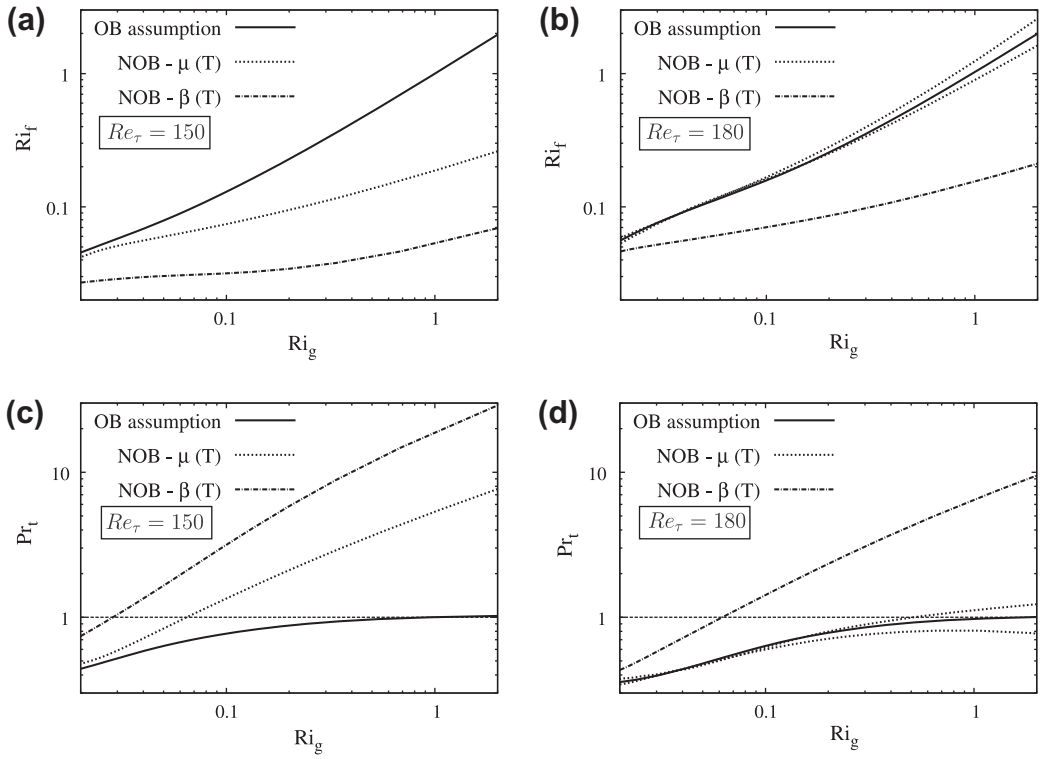

Fig. 4. Mixing efficiency (Ri_f) and turbulent Prandtl number (Pr_t) as a function of the gradient Richardson number Ri_g: (a) Ri_f for simulations of stratified turbulence at $Re_\tau = 150$ ($Ri_\tau = 498$). (b) Ri_f for simulations of stratified turbulence at $Re_\tau = 180$ ($Ri_\tau = 326$). (c) Pr_t for simulations of stratified turbulence at $Re_\tau = 150$ ($Ri_\tau = 498$). (d) Pr_t for simulations of stratified turbulence at $Re_\tau = 180$ ($Ri_\tau = 326$). Results obtained using OB assumption (solid line) are compared with those obtained using $\mu(T)$ (dotted line) and $\beta(T)$ (dash-dotted line).

where B_k and P_k are production of Turbulent Kinetic Energy (TKE) by buoyancy and by mean shear, respectively. Mixing efficiency quantifies the amount of TKE (which, from a theoretical point of view, is the energy available for mixing) lost to Potential Energy (PE). The behaviour of Ri_f is shown in Fig. 4a and b as a function of the gradient Richardson number, $Ri_g = g\beta(\partial\langle\theta\rangle/\partial z)/(\partial\langle u_x\rangle/\partial z)^2$. Note that computation of Ri_f is possible for $Ri_\tau = 498$ ($Re_\tau = 150$) and $Ri_\tau = 346$ ($Re_\tau = 180$) only, since for $Ri_\tau = 926$ ($Re_\tau = 110$) the flow is laminar. Under OB conditions, Ri_f increases almost linearly with Ri_g for both $Re_\tau = 150$ and $Re_\tau = 180$ (solid lines in Fig. 4a and b). When $Ri_f < 1$, the shear production of turbulence (P_k) dominates, and the usual turbulent boundary layer theory applies (in the near wall region, a small fraction of TKE is lost to PE). When $Ri_f > 1$, we expect the buoyancy flux (B_k) to suppress the boundary layer turbulence. This happens in the core region of the channel, where a large proportion of TKE is lost to PE owing to IGW (thermocline). Under NOB conditions ($\mu(T)$ and $\beta(T)$), Ri_f was computed only for the turbulent region of the channel: for the laminar region there is no production of TKE by either shear, $P_k \to 0$, or buoyancy, $B_k \to 0$. Fig. 4a and b show that Ri_f decreases strongly for both $Re_\tau = 150$ and $Re_\tau = 180$, meaning that turbulence is mainly produced by shear and only a small proportion of TKE is lost to PE ($Ri_f < 1$). This is true except for the case of $\mu(T)$ and $Re_\tau = 180$. For this situation, Ri_f is close to the value computed for OB assumptions (no laminarization is observed and the flow structure is similar to the OB case).

To investigate further on mixing and energy transfer mechanisms in stratified turbulence, we computed the turbulent Prandtl number Pr_t. Within the framework of the eddy viscosity hypothesis,

$$\langle u_x' u_z' \rangle = D_u \frac{\partial\langle u_x\rangle}{\partial z}, \quad \langle \theta' u_z' \rangle = D_\theta \frac{\partial\langle\theta\rangle}{\partial z}, \tag{8}$$

where u_z' is the fluctuation of the wall-normal velocity while D_u and D_θ are the eddy diffusivities for momentum and heat transfer (introduced to obtained a simple relationship between the extra shear stress and the heat flux in turbulent flows). Therefore, the turbulent Prandtl number is defined as

$$Pr_t = \frac{D_u}{D_\theta} = \frac{Ri_g}{Ri_f}. \tag{9}$$

The behaviour of Pr_t is shown in Fig. 4c and d as a function of Ri_g for stratified turbulence at $Re_\tau = 150$ (Fig. 4c) and and $Re_\tau = 180$ (Fig. 4d). Under OB conditions, $Pr_t \simeq 1$ with a slight increase observed for increasing Ri_g. This result is in fair agreement with previous studies, where $0.7 < Pr_t < 1.2$ depending on the specific flow configuration (Gerz et al., 1989; Armenio and Sarkar, 2002). Under NOB conditions a different behaviour is observed for Pr_t, which attains larger values (associated to lower values of Ri_f). For these situations, increase of Pr_t with Ri_g is almost linear and does not attain an asymptotic value. We note that NOB effects induced by $\mu(T)$ weaken for the case of $Re_\tau = 180$ (dotted lines in Fig. 4b and d), owing to the Re_τ^{-1} scaling of the viscous term (Zonta et al., 2012a). Non-uniform Pr_t may be an issue in RANS modelling, where the Reynolds analogy ($Pr_t = 1$) is widely used (Laskowski et al., 2007). Although this analogy holds in several flow instances (boundary layers, pipes), it is difficult to extend its validity to more complex flows (i.e. stratified flows). Here we have shown that the assumption $Pr_t = 1$ is reasonable for stratified turbulence under OB conditions only, but it is unphysical and inaccurate under NOB conditions. More accurate physical modelling is thus required to improve current parametrization of mixing in stratified turbulence.

4. Conclusions

We have used DNS to evaluate NOB effects on momentum and heat transfer mechanisms for stably-stratified turbulence in water flows. Under NOB conditions, significant changes on the flow

structure may occur. In particular, one-sided turbulence with local flow laminarization may be observed, depending on the flow parameters (Re_τ,Ri_τ). Associated to changes of the local flow structure, large variations of heat (Nu) and momentum transfer coefficients (C_f) may be observed. Since evaluating heat transfer rates in stratified turbulence is of fundamental importance for environmental and industrial problems, we have developed a phenomenological model for Nu prediction as a function of Re_τ and Ri_τ (for both OB and NOB conditions). We have also discussed the implication of NOB conditions on mixing efficiency (i.e. flux Richardson number Ri_f) and turbulent Prandtl number (Pr_t). We have demonstrated that the widely-used Reynolds analogy $Pr_t = 1$ (RANS modelling) may be applied to stratified turbulence only under OB assumptions. For all those situations in which NOB effects become significant, the Reynolds analogy is not justified and accurate physical modelling is required to improve parametrization of mixing. Extensions of the present results to cover a larger range of Reynolds/Richardson numbers will be the subject of future works.

Acknowledgements

The author gratefully acknowledge Prof. A. Soldati and Dr. C. Marchioli for helpful discussion during the preparation of the manuscript. CINECA supercomputing centre (Bologna, Italy) and DEISA Extreme Computing Initiative are gratefully acknowledged for generous allowance of computer resources. Support from PRIN (under Grant 2006098584_004) and from HPC Europa Transnational Access Program (under Grants 466 and 708) are gratefully acknowledged.

References

Ahlers, G., Brown, E., Araujo, F.F., Funfschilling, D., Grossmann, S., Lohse, D., 2006. Non-Oberbeck–Boussinesq effects in strongly turbulent Rayleigh–Benard convection. J. Fluid Mech. 569, 409.

Ahlers, G., Grossmann, S., Lohse, D., 2009. Heat transfer and large scale dynamics in turbulent Rayleigh–Benard convection. Rev. Mod. Phys. 81, 503.

Armenio, V., Sarkar, S., 2002. An investigation of stably stratified turbulent channel flow using large-eddy simulation. J. Fluid Mech. 459, 1.

Arya, S.P.S., 1975. Buoyancy effects in an horizontal flat-plate boundary layer. J. Fluid Mech. 68, 321.

Dean, R.B., 1978. Reynolds number dependence of skin friction and other bulk flow variables in two-dimensional rectangular duct flow. ASME J. Fluid Eng. 100, 215.

Ferziger, J.H., Koseff, J.R., Monismith, S.G., 2002. Numerical simulation of geophysical turbulence. Comput. Fluids 31, 557.

Gerz, T., Schumann, U., Elghobashi, S.E., 1989. Direct numerical simulation of stratified homogeneous turbulent shear flows. J. Fluid Mech. 200, 563.

Hetsroni, G., Kaftori, D., Yarin, L.P., 1996. A mechanistic model for heat transfer from a wall to a fluid. Int. J. Heat Mass Transfer 39, 1475.

Iida, O., Kasagi, N., Nagano, Y., 2002. Direct numerical simulation of turbulent channel flow under stable density stratification. Int. J. Heat Mass Transfer 45, 1693.

Incropera, F.P., Dewitt, D.P., 1985. Fundamentals of Heat and Mass Transfer. John Wiley and Sons Inc., New York.

Laskowski, G.M., Kearney, S.P., Evans, G., Greif, R., 2007. Mixed convection heat transfer to and from a horizontal cylinder in cross-flow with heating from below. Int. J. Heat Fluid Flow 28, 454.

Peltier, W.R., Caulfield, C.P., 2003. Mixing efficiency in stratified shear flows. Annu. Rev. Fluid Mech. 35, 135.

Sameen, A., Verzicco, R., Sreenivasan, K.R., 2009. Specific role of fluid properties in non-Boussinesq thermal convection at the Rayleigh number of 2×10^8. Europhys. Lett. 86, 14006.

Schlichting, H., 1979. Boundary Layer Theory. McGraw-Hill, New York.

Sieder, E.N., Tate, G.E., 1936. Heat transfer and pressure drop of liquids in tubes. Ind. Eng. Chem. 28, 1429.

Sugiyama, K., Calzavarini, E., Grossmann, S., Lohse, D., 2009. Flow organization in two-dimensional non-Oberbeck–Boussinesq Rayleigh–Bénard convection in water. J. Fluid Mech. 637, 105.

Zonta, F., Soldati, A., 2013. Effect of temperature dependent fluid properties on heat transfer in turbulent mixed convection. J. Heat Transfer – Trans. ASME (in press).

Zonta, F., Marchioli, C., Soldati, A., 2012a. Modulation of turbulence in forced convection by temperature-dependent viscosity. J. Fluid Mech. 697, 150.

Zonta, F., Onorato, M., Soldati, A., 2012b. Turbulence and internal waves in stably-stratified channel flow with temperature-dependent fluid properties. J. Fluid Mech. 697, 175.